THE
PHYSICAL REVIEW

A journal of experimental and theoretical physics established by E. L. Nichols in 1893

SECOND SERIES, VOL. 124, NO. 5 DECEMBER 1, 1961

Absorption of Electromagnetic Radiation by an Electron Gas*

NARKIS TZOAR† AND ABRAHAM KLEIN
University of Pennsylvania, Philadelphia, Pennsylvania
(Received June 5, 1961)

The total absorption cross section for a photon by an electron gas is calculated in the high-density limit. The calculation makes use of the Green's function formulation of the many-body problem. Only the simplest final states leading to a nonvanishing cross section, consisting of an electron-hole pair and a plasmon, are taken into account. This contribution has a threshold near the plasmon energy and is peaked owing to the initially rapid rise of the available phase space, with a total cross section for real metals of $10^{-17}-10^{-19}$ cm^2 per electron. This compares favorably with other absorption mechanisms.

I. INTRODUCTION

MUCH progress has been made in the theory of the many-body problem during the last several years.[1] In particular, from the point of view of perturbation theory, we have learned how to select and calculate those terms (diagrams) for many physical quantities which give the most important contributions in the high- and low-density limits. In this work we shall be interested mostly in the high-density limit, which in application to electron gases in metals has served to illuminate some important features of their behavior. In particular the existence of plasmons in metals indicates that the long-range correlations emphasized by the high-density approximation still play an important role, although electron gases in metals cannot truly be classified as high-density gases.

The fundamental advance in the treatment of this limit[2] came with the realization that the leading contributions arise from matrix elements, of whatever order in the coupling, in which the interaction always transfers the same momentum, and that these contributions can be summed.

Before going on to discuss the extension of this idea with which the present work is concerned, we shall entertain a brief outline of the present status,[3] partly to establish the language and notation with which we shall work. We consider a Hamiltonian for the many-fermion system of the form

$$H_0=H_{00}+H_I, \tag{1}$$

where

$$H_{00}=\int d\mathbf{x}\,\psi^\dagger(\mathbf{x})(-\nabla^2)\psi(\mathbf{x}),$$
$$H_I=\frac{\lambda}{2}\int\int d\mathbf{x}d\mathbf{x}'\,v(\mathbf{x}-\mathbf{x}')\psi^\dagger(\mathbf{x})\psi^\dagger(\mathbf{x}')\psi(\mathbf{x}')\psi(\mathbf{x}), \tag{2}$$

and $\psi(\mathbf{x})$ and $\psi^\dagger(\mathbf{x})$ are, respectively, the fermion destruction and creation operators with spin indices omitted. These operators obey the usual anticommutation relations

$$[\psi(\mathbf{x}),\psi^\dagger(\mathbf{x}')]_+=\delta(\mathbf{x}-\mathbf{x}'),$$
$$[\psi(\mathbf{x}),\psi(\mathbf{x}')]_+=[\psi^\dagger(\mathbf{x}),\psi^\dagger(\mathbf{x}')]_+=0. \tag{3}$$

As is well known, and as will be illustrated again in the following pages, many of the observables of interest can be related to the propagators or Green's functions for one and two particles.[3] We follow the notation and

* Supported in part by the U. S. Atomic Energy Commission.
† Present Address: Physics Department, Columbia University New York, New York.

[1] For a general review see *The Many-Body Problem*, edited by C. Dewitt (John Wiley & Sons, Inc., New York, 1959).

[2] M. Gell-Mann and K. A. Brueckner, Phys. Rev. **106**, 364 (1957); K. Sawada, *ibid.* **106**, 372 (1957); K. Sawada, K. A. Brueckner, N. Fukuda and R. Brout, *ibid.* **108**, 507 (1957); J. Hubbard, Proc. Roy. Soc. (London) **A240**, 539 (1957); **A243**, 336 (1958); D. Bohm and D. Pines, Phys. Rev. **82**, 625 (1951); **85**, 332 (1952); **92**, 609 (1953); D. Pines, *ibid.* **92**, 626 (1954); P. Nozières and D. Pines, Nuovo cimento **9**, 470 (1958). D. F. DuBois, Ann. Phys. **7**, 174 (1959), **8**, 24 (1959). H. Kanazawa, S. Misawa and E. Fujita, Prog. Theoret. Phys. (Kyoto) **23**, 426 (1960).

[3] A. Klein and R. Prange, Phys. Rev. **112**, 994 (1958); V. M. Galitskii and A. B. Migdal, Soviet Phys. J.E.T.P. **34**, No. 1, 139 (1958); P. Martin and J. Schwinger, Phys. Rev. **115**, 1342 (1959); H. Kanazawa and M. Watabe, Progr. Theoret. Phys. (Kyoto) **23**, 408 (1960); D. F. DuBois, Ann. Phys. **7**, 174 (1959); **8**, 24 (1959).

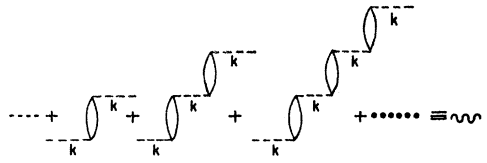

FIG. 1. Representation by Feynman diagrams of the sum of matrix elements which defines the effective or screened interaction.

definitions in the paper of Klein and Prange,[3] defining

$$G(x-x')=i\langle 0|\,T\{\psi(x)\psi^\dagger(x')\}\,|0\rangle=G(x\,|\,x'),$$
$$G(xx'\,|\,yy')=i^2\langle 0|\,T\{\psi(x)\psi(x')\psi^\dagger(y')\psi^\dagger(y)\}\,|0\rangle. \quad (4)$$

Here $|0\rangle$ is the exact ground state of the Hamiltonian H_0, and T is the usual time-ordering operator, and the symbol x stands for $(\mathbf{x},t)$.

For example, the ground-state energy of an interacting fermion gas is given by

$$E(N,0)=E_0(N,0)+\tfrac{1}{2}(-i)^2\int_0^\lambda\frac{d\lambda'}{\lambda'}\int d\mathbf{r}\int d\mathbf{r}'\times\lim_{t'\to t+}v(\mathbf{r}-\mathbf{r}')G(\mathbf{r}t,\mathbf{r}'t'\,|\,\mathbf{r}t',\mathbf{r}t')$$
$$=E_0(N,0)+\tfrac{1}{2}(-i)^2\int_0^\lambda\frac{d\lambda'}{\lambda'}\times\sum_{\mathbf{p}\mathbf{p}'\mathbf{q}}v_q\lim_{t'\to t+}G(\mathbf{p}t,\mathbf{p}'t\,|\,\mathbf{p}+\mathbf{q}\,t',\mathbf{p}'-\mathbf{q}\,t'), \quad (5)$$

where $E_0(N,0)$ is the ground-state energy of the noninteracting gas, i.e., of the filled Fermi sphere. As a second example the distribution of particles in momentum space is given by

$$N(\mathbf{p})=\lim_{t\to 0+}\frac{1}{2\pi i}\int_{-\infty}^{+\infty}dp_0\exp(-ip_0t)G(\mathbf{p},p_0), \quad (6)$$

where $G(\mathbf{p},p_0)$ is the Fourier transform of $G(\mathbf{x},t)$.

In studying these quantities, we shall use the method of power-series expansion and (where necessary) selective resummation of terms. In so doing, we shall employ extensively the representation by Feynman graphs, and the associated rules for recording of matrix elements as given, for example, in the first paper of reference 3.

As an essential ingredient of these expansions there then occurs the one-particle Green's function for a noninteracting particle,

$$G(\mathbf{x},t)=\frac{i}{\Omega}\sum_{\mathbf{p}}[\theta_F(\mathbf{p})\theta(t)-\bar\theta_F(\mathbf{p})\bar\theta(t)]\times\exp(i\mathbf{p}\cdot\mathbf{x}-ip^2t), \quad (7)$$

where $\bar\theta_F(\mathbf{p})=1-\theta_F(\mathbf{p})$, etc. The Fourier transform of $G(\mathbf{x},t)$ is given by

$$G(\mathbf{p},p_0)=\frac{\theta_F(\mathbf{p})}{-p_0+p^2-i\eta}+\frac{\bar\theta_F(\mathbf{p})}{-p_0+p^2+i\eta}. \quad (8)$$

We return now to a description of the diagrams which contribute most to the one- and two-particle Green's functions in the high-density limit. As was shown in reference 2, we must consider mainly the ring diagrams. These are summed by means of the effective interaction, which is given by the sum represented in Fig. 1 by a wavy line. This sum acts, for many purposes, like a boson propagator.

As a first illustration of its use we consider the lowest correction to the free-electron propagator in a dense gas. This is provided by the diagram of Fig. 2, and it is immediately obtained according to the above discussion.[4] As a second example, we consider the correlation energy, ΔE, of the ground state[5] (exclusive of the exchange contribution). This is given in terms of the particle-hole propagator which is a particular case of the two-particle Green's function. In order to compute ΔE for the dense gas we must sum over all the diagrams indicated in Fig. 3(a). Using the definition of the effective potential we obtain the result illustrated by the diagram of Fig. 3(b).[6]

We are now prepared to illustrate the method for choosing the important diagrams for the problem of interest in this work. Let us consider the high density approximation for the followlng process: A photon or external field excites a particle-hole pair in the electron gas. The pair propagates, undergoing all kinds of interaction with itself and with the rest of the electron gas. The excitation finally disappears by means of a second electromagnetic interaction.

As we shall see in Sec. II, the above description applies, among others, to the total cross section for photon absorption by the electromagnetic field which we shall wish to calculate. We thus have a process of second order in the external field, of which a diagrammatic representation is achieved by taking all vacuum-to-vacuum diagrams and inserting a pair of crosses either in any of the electron lines or in place of any of the

FIG. 2. Diagrammatic representation of the leading correction, in the high-density limit, to the free electron propagator.

[4] The most complete discussion of the plasmon similar to our point of view is given in the papers of D. F. DuBois mentioned in reference 2. See also J. Lindhard, Kgl. Danske Videnskab. Selskab, Mat-fys. Medd. **28**, No. 8, (1954); J. Hubbard, Proc. Roy. Soc. (London) **A240**, 539 (1957); **A234**, 336 (1958).

[5] A complete discussion of the correlation energy can be found in the papers by Bohm and Pines, Gell-Mann and Brueckner, Sawada *et al.*, and Dubois mentioned in reference 2.

[6] We consider here only the ring diagrams even though we have an additional contribution to the correlation energy from one exchange diagram.

interaction lines. We immediately observe, for example, that there are only three basically different second order diagrams which exhibit the same momentum transfer in each of their interaction lines. These are illustrated by Fig. 4.

Proceeding to higher order, one finds that the major contribution to each order results from three similar diagrams. Their sum is given in Figs. 5(a)–(c). The contribution from the diagram in Fig. 5(c) alone constitutes the random-phase approximation.[7] In the high-density limit it represents the most important contribution, since, unlike the other two diagrams in Fig. 5, which depend on electron and/or hole scattering matrix elements, it contains only the electron-hole pair creation and annihilation parts of H_I.

It is, of course, well known by now that a theory which includes only the latter matrix elements leads precisely to the random-phase approximation, which can be characterized equally well as the one-pair approximation. Since also the effective potential is generated by pair fluctuations, the contributions from Figs. 5(a) and (b) go beyond this approximation.

As intimated above, the diagrams of Fig. 5 are meant to represent contributions to the *cross section* for photon absorption. The final state contributing to the matrix element is obtained by cutting the diagram in two with a horizontal slice. At this point we must recall that the cut effective potential line represents either a free-pair or a plasmon (bound-pair) final state. Where this represents the full final state, the corresponding matrix element vanishes, indeed for two reasons, because of energy-momentum conservation, and because the longitudinal plasmon cannot be excited by the transverse photon.

We must then study the contributions of Figs. 5(a), (b) which correspond to final states of two pairs, one of which may be bound. Insofar as our theory goes beyond the simplest high-density limit, it will represent a further test of the applicability to real metals of the plasmon concept which emerges in this limit.

In the work which follows we shall calculate that contribution to the photon absorption cross section, in which one of the pairs is a free pair while the other represents the pair bound state or plasmon. For this case we shall obtain a cross section which has a threshold at

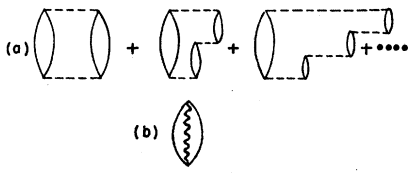

FIG. 3. Contributions to the correlation energy in the high-density limit.

[7] It should be emphasized that throughout we use the term R.P.A. in a primitive but precisely defined sense. Recently the term generalized R.P.A. has been introduced to characterize a more inclusive approximation, arising from a linearization of the field equations. In the latter approximation, the cross section would not vanish.

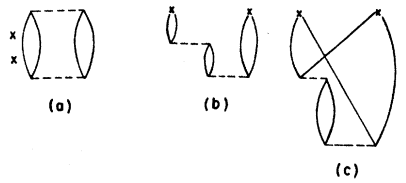

FIG. 4. Contributions to the absorption cross section for light by an electron gas of second order in the particle–particle interaction.

a photon energy equal to the plasmon energy, thereafter rising to a peak and then tailing off as ω^{-2}, where ω is the photon energy. This calculated cross section will therefore exhibit a peak in the absorption cross section per particle which may be detectable experimentally, as discussed in more detail in the concluding section.

II. PHOTON-ABSORPTION CROSS SECTION; HIGH-DENSITY LIMIT

In this section we develop a formula for the total cross section for absorption of light by an electron gas, to the lowest order in the electromagnetic field, while taking into account as exactly as possible the properties of the electron gas.

The Hamiltonian which describes the above process is

$$H=H_0+H', \tag{9}$$

where

$$H_0=\int d\mathbf{x}\,\psi^\dagger(\mathbf{x})(-\nabla^2)\psi(\mathbf{x})+\frac{1}{2}\int\int d\mathbf{x}d\mathbf{x}'\,v(\mathbf{x}-\mathbf{x}')\times\psi^\dagger(\mathbf{x})\psi^\dagger(\mathbf{x}')\psi(\mathbf{x}')\psi(\mathbf{x}),$$
$$H'=-\frac{1}{c}\int\mathbf{j}(\mathbf{x})\cdot\mathbf{A}(\mathbf{x})d\mathbf{x}, \tag{10}$$

and where the current $\mathbf{j}$ is given by

$$\mathbf{j}(\mathbf{x})=ie\{\nabla\psi^\dagger(\mathbf{x})\psi(\mathbf{x})-\psi^\dagger(\mathbf{x})\nabla\psi(\mathbf{x})\}. \tag{11}$$

In Eq. (11) we have neglected the term in $\mathbf{j}$ which is proportional to e^2. We are using the natural units $2m=\hbar=1$.

The total-absorption cross section of a photon by an electron gas is

$$\sigma=\frac{2\pi}{c}\frac{1}{2\omega}\sum_{N'}\int d\mathbf{x}\int d\mathbf{x}'\,\delta(E_{N'}-E_N-\omega)\times\exp[-i\mathbf{k}\cdot(\mathbf{x}-\mathbf{x}')]e_i(k\lambda)e_j(k\lambda)\times\langle N0|\,j_i(\mathbf{x})\,|N'\rangle\langle N'|\,j_j(\mathbf{x}')\,|N0\rangle. \tag{12}$$

FIG. 5. Leading contributions to the absorption cross section for light by an electron gas in the high-density limit.

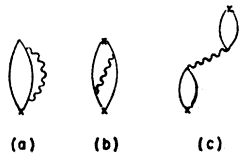

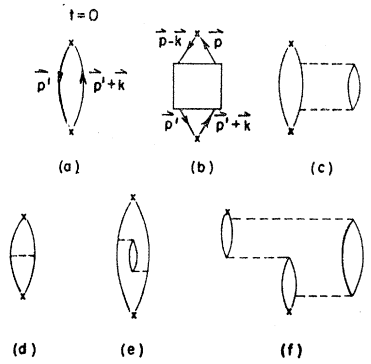

FIG. 6. Some contributions to the absorption cross section for light by an electron gas.

Here $|N'\rangle$, $E_{N'}$ represent, respectively, any excited state of the electron gas; $\mathbf{k}$ is the photon momentum, ω its energy, and $\mathbf{e}(k\lambda)$ its polarization vector ($\mathbf{e}\cdot\mathbf{k}=0$).

In order to sum over the excited states N', we use the Fourier transform for the Dirac δ function and also the invariance of $\langle N0|\, j_i(\mathbf{x})j_j(\mathbf{x}'\tau)\,|N0\rangle$ under time translation to obtain

$$\sigma=\sigma_A+\sigma_A{}^*=2\,\mathrm{Re}\sigma_A, \tag{13}$$

where

$$\sigma_A=\frac{1}{2\omega c}\int d\mathbf{x}\int d\mathbf{x}'\int_{-\infty}^{0}d\tau\,\exp(-i\omega\tau)\times\exp[-i\mathbf{k}\cdot(\mathbf{x}-\mathbf{x}')]e_i(k\lambda)e_j(k\lambda)\times\langle N0|\, j_i(\mathbf{x})j_j(\mathbf{x}',\tau)\,|N0\rangle. \tag{14}$$

We now use the definitions of Eqs. (4) and (12) to express the cross section in term of the two-particle Green's function. We thus obtain

$$\sigma_A=\frac{e^2}{2\omega c}\int d\mathbf{x}\int d\mathbf{x}'\int_{-\infty}^{0}d\tau\,\exp(-i\omega\tau)\times\exp[-i\mathbf{k}\cdot(\mathbf{x}-\mathbf{x}')]e_i(k\lambda)e_j(k\lambda)\times\mathrm{Lim}\left(\frac{\partial}{\partial y_i}-\frac{\partial}{\partial x_i}\right)\left(\frac{\partial}{\partial y_j'}-\frac{\partial}{\partial x_j'}\right)G(xx'|\,yy'), \tag{15}$$

where

$$\mathrm{Lim}\equiv\lim_{\substack{y_0>x_0=0>y_0'>x_0'=\tau\\ \mathbf{y},\mathbf{y}',y_0,y_0'\to\mathbf{x},\mathbf{x}',x_0,x_0'}}.$$

To obtain the more familiar momentum representation form for σ_A, we express the above two-particle Green's function in terms of its Fourier transform. Then, we carry out the integration over $\mathbf{x}$ and $\mathbf{x}'$. This yields the following expression for σ_A:

$$\sigma_A=-\frac{2e^2}{\omega c}\sum_{\mathbf{pp}'}[\mathbf{e}(k\lambda)\cdot\mathbf{p}][\mathbf{e}(k\lambda)\cdot\mathbf{p}']\times\int_{-\infty}^{0}d\tau\,\exp(-i\omega\tau)\times G(\mathbf{p}0,\,\mathbf{p}'\tau|\,\mathbf{p}-\mathbf{k}\,0_+,\,\mathbf{p}'+\mathbf{k}\,\tau_+), \tag{16}$$

where 0_+, τ_+ means the approach from more positive values.

In Eq. (16), if we sum over initial polarization we obtain

$$\sum_{\mathrm{pol}}[\mathbf{e}(k\lambda)\cdot\mathbf{p}][\mathbf{e}(k\lambda)\cdot\mathbf{p}']=\mathbf{p}\cdot\mathbf{p}'-(\mathbf{p}\cdot\hat{k})(\mathbf{p}'\cdot\hat{k}), \tag{17}$$

where $\hat{k}$ is a unit vector in the direction of $\mathbf{k}$.

We now turn to the calculation of the two-particle Green's function for the special case of a dense electron gas. We first consider the zero-order approximation, that is, the absence of interaction between the electrons. In this case the two-particle Green's function is given by

$$G(\mathbf{x}0|\,\mathbf{y}0_+)G(\mathbf{x}'\tau|\,\mathbf{y}'\tau_+)-G(\mathbf{x}0|\,\mathbf{y}'\tau)G(\mathbf{x}'\tau|\,\mathbf{y}0). \tag{18}$$

The first of these terms does not contribute to the cross section, as the terms arising here do not permit energy transfer to the matter system. As for the second, or exchange term, its Fourier transform is given by the expression

$$-\frac{1}{(2\pi)^2}\frac{\Omega}{(2\pi)^3}\int dq_0dq_0'\,\exp[i\tau(q_0-q_0')]\times G(\mathbf{p}',q_0')G(\mathbf{p},q_0)\delta(\mathbf{p}'-\mathbf{p}-\mathbf{k}), \tag{19}$$

and its possible contribution to the cross section illustrated in Fig. 6(a). Here the "cross" at $t=\tau$ describes the transfer of momentum $\mathbf{k}$ to the system of the electron gas by the photon and the creation of a pair. The "cross" at $t=0$ describes the annihilation of the pair which gives its momentum back to the photon.

The first-order diagram is given in Fig. 6(b), and represents a single interaction between the two-fermion propagators. Similarly, the nth order diagram will be any diagram including n interactions (represented by n dotted lines). Some of these diagrams are shown in Fig. 6(c), (d), (e). The rules for building the two-particle Green's function for these diagrams are identical to those given by Klein and Prange.[3] In order to obtain the cross section we must first multiply the two-particle Green's function by the factor $(\mathbf{e}\cdot\mathbf{p})(\mathbf{e}\cdot\mathbf{p}')$ represented symbolically in the diagrams by the crosses, and then sum over the momenta $\mathbf{p}$ and $\mathbf{p}'$.

Of course the contribution from diagram 6(a) vanishes identically since it corresponds to a final state consisting of a free electron-hole pair which cannot simultaneously conserve energy and momentum. Many higher order diagrams, as we shall see below, will vanish for the same reason. [All this can be shown directly from expression (16), of course. The inclusion of vanishing matrix elements is a consequence of the technique for writing the cross section in terms of the two-particle Green's function.]

We turn now to a study of the high-density limit. Following our discussion in the introduction we are looking for contributions to the two-particle Green's function given by the diagrams in Figs. 5(a)–(c). We

first notice that the effective potential defined before as the sum of contributions of the diagrams in Fig. 1 can be represented by an integral equation

$$V(z-z')=iv(\mathbf{z}-\mathbf{z}')-\int iv(\mathbf{z}-\mathbf{x})G(x-y)\times G(y-x)V(y-z')d\mathbf{x}d^4y. \quad (20)$$

The Fourier transform of V is given by

$$U(\mathbf{q},q_0)=iv(\mathbf{q})/[1+v(\mathbf{q})Q(\mathbf{q},q_0)], \quad (21)$$

which constitutes the solution of (20), where

$$Q(\mathbf{q},q_0)=\frac{i}{(2\pi)^4}\int d\mathbf{p}dp_0\, G(\mathbf{p},p_0)G(\mathbf{p}+\mathbf{q},\, p_0+q_0). \quad (22)$$

The function Q in Eq. (22) represents the density fluctuation function.

The first-order contribution to the cross section is now given by setting G_{12}, the two-particle Green's function, equal to these contributions which are obtained by letting the effective potential act once. These are the contributions shown in Figs. 7(a)–(d). The diagram in Fig. 7(a) represents the contribution from the random-phase approximation; as we now show, however, the contribution to the cross section from this diagram vanishes. This conclusion is based on the fact that although in general $\sigma_A \propto \int (\mathbf{e}\cdot\mathbf{p})(\mathbf{e}\cdot\mathbf{p}')d\mathbf{p}d\mathbf{p}'G_{12}(\mathbf{p}\mathbf{p}'\mathbf{k})$, we have from diagram (7a) a contribution to G_{12} in the separable form $G_{12}=F(\mathbf{p}\mathbf{k})F(\mathbf{p}'\mathbf{k})$. Since necessarily

$$\int d\mathbf{p}\ \mathbf{p}F(\mathbf{p}\mathbf{k})=A(k^2)\mathbf{k},$$

and $(\mathbf{e}\cdot\mathbf{k})=0$, the contribution to σ_A from diagram 7(a) is zero. We can conclude, therefore, that the random-phase approximation, and any corrections which can be described in the most general way by the diagram of Fig. 7(e), do not contribute to the process of the absorption of light. As we shall remark again later, these contributions also vanish because they cannot lead to any energy-momentum conserving final states.

We now calculate the contribution to the cross section from the approximate G_{12} as it is represented by diagrams 7(b)–(d). By performing a routine calculation we obtain the contributions:

$$\sigma_A(b)=\frac{2e^2}{\omega c}\frac{1}{(2\pi)^6}\frac{\Omega}{(2\pi)^3}\int d\mathbf{p}'(\mathbf{e}\cdot\mathbf{p}')^2\times\int_{-\infty}^{0}d\tau\exp(-i\omega\tau)\int dq_0dq_0'd\mathbf{s}ds_0\, G(\mathbf{p}'+\mathbf{k},\, q_0)\times G(\mathbf{p}'+\mathbf{k}+\mathbf{s},\, q_0+s_0)G(\mathbf{p}'+\mathbf{k},\, q_0)\times G(\mathbf{p}',q_0')U(\mathbf{s},s_0)\exp[i\tau(q_0-q_0')], \quad (23)$$

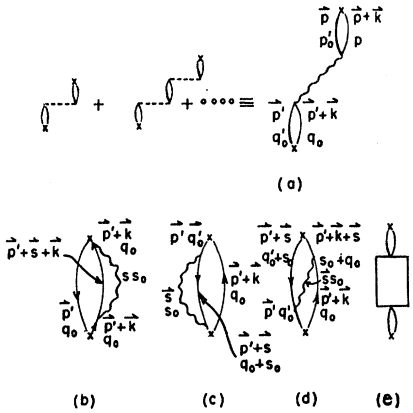

FIG. 7. More detailed representation of the high-density approximation to the absorption cross section.

$$\sigma_A(c)=\frac{2e^2}{\omega c}\frac{1}{(2\pi)^6}\frac{\Omega}{(2\pi)^3}\int d\mathbf{p}'(\mathbf{e}\cdot\mathbf{p}')^2\times\int_{-\infty}^{0}d\tau\exp(-i\omega\tau)\int dq_0dq_0'd\mathbf{s}ds_0\, G(\mathbf{p}'+\mathbf{k},\, q_0)\times G(\mathbf{p}',q_0')G(\mathbf{p}'+\mathbf{s},\, q_0+s_0)\times G(\mathbf{p}',q_0')U(\mathbf{s},s_0)\exp[i\tau(q_0-q_0')], \quad (24)$$

$$\sigma_A(d)=\frac{2e^2}{\omega c}\frac{1}{(2\pi)^6}\frac{\Omega}{(2\pi)^3}\int d\mathbf{p}'d\mathbf{s}(\mathbf{e}\cdot\mathbf{p}')\times(\mathbf{e}\cdot[\mathbf{p}'+\mathbf{s}])\int_{-\infty}^{0}d\tau\exp(-i\omega\tau)\times\int dq_0dq_0'ds_0\, G(\mathbf{p}',q_0')G(\mathbf{p}'+\mathbf{s},\, q_0'+s_0)\times G(\mathbf{p}'+\mathbf{k},\, q_0)G(\mathbf{p}'+\mathbf{k}+\mathbf{s},\, q_0+s_0)\times U(\mathbf{s},s_0)\exp[i\tau(q_0-q_0')]. \quad (25)$$

We now calculate $\sigma_A(d)$ in detail. The calculation of $\sigma_A(b)$ and $\sigma_A(c)$ can be done similarly. Integrating first over τ we obtain

$$\sigma_A(d)=\frac{2e^2}{\omega c}\frac{1}{(2\pi)^6}\frac{\Omega}{(2\pi)^3}\int d\mathbf{p}'d\mathbf{s}(\mathbf{e}\cdot\mathbf{p}')\times[\mathbf{e}\cdot(\mathbf{p}'+\mathbf{s})]\int dq_0dq_0'ds_0\, U(\mathbf{s},s_0)\times\frac{-i}{q_0-q_0'-\omega-i\eta}G(\mathbf{p}',q_0')G(\mathbf{p}'+\mathbf{k},\, q_0)\times G(\mathbf{p}'+\mathbf{s},\, q_0'+s_0)G(\mathbf{p}'+\mathbf{k}+\mathbf{s},\, q_0+s_0). \quad (26)$$

Here the one-particle Green's function is given by

$$G(\mathbf{p},p_0)=\frac{\theta_F(\mathbf{p})}{-p_0+p^2-i\eta}+\frac{\bar{\theta}_F(\mathbf{p})}{-p_0+p^2+i\eta}. \quad (27)$$

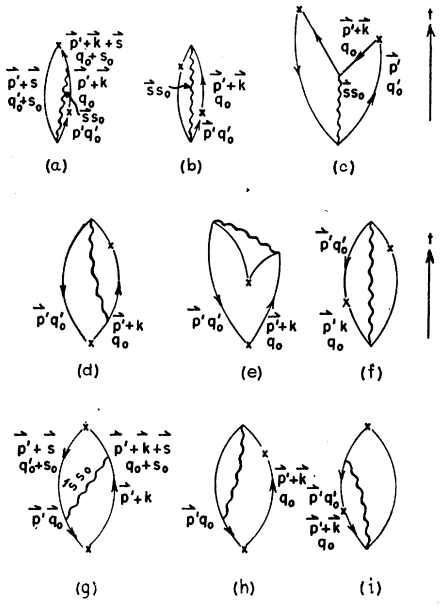

FIG. 8. Time-ordered contributions to the Feynman diagram of Fig. 7(d).

It is convenient to have also the separate definitions

$$G^{+}(\mathbf{p},p_0)=\frac{\theta_F(\mathbf{p})}{-p_0+p^2-i\eta};\quad G^{-}(\mathbf{p}p_0)=\frac{\bar{\theta}_F(\mathbf{p})}{-p_0+p^2+i\eta}. \tag{28}$$

By studying the poles in the variables q_0 and q_0' we arrive at the result that $\sigma_A(d)$ may be written as a sum of the nine time-dependent diagrams of Fig. 8. For these diagrams we must represent any line going in the direction of increasing time by G^{+} and any line going in the opposite direction by G^{-}. The calculation of the contribution from any one of the nine diagrams is sufficient to illustrate method. We therefore choose to calculate in detail the contribution of Fig. 8(a). We obtain

$$\begin{aligned}\sigma_A^{(1)}(d)=&\frac{2e^2}{\omega c}\frac{1}{(2\pi)^6}\frac{\Omega}{(2\pi)^3}\int d\mathbf{p}'d\mathbf{s}(\mathbf{e}\cdot\mathbf{p}')[\mathbf{e}\cdot(\mathbf{p}'+\mathbf{s})]\\&\times(-i)\theta_F(\mathbf{p}')\theta_F(\mathbf{p}'+\mathbf{k})\theta_F(\mathbf{p}'+\mathbf{k}+\mathbf{s})\\&\times\bar{\theta}_F(\mathbf{p}'+\mathbf{s})\int ds_0dq_0dq_0'\,U(\mathbf{s},s_0)\\&\times\frac{1}{q_0-q_0'-\omega-i\eta}\frac{1}{-q_0'+\epsilon_{p'}-i\eta}\\&\times\frac{1}{-q_0+\epsilon_{p'+k}-i\eta}\frac{1}{-q_0-s_0+\epsilon_{p'+s+k}-i\eta}\\&\times\frac{1}{-q_0'-s_0+\epsilon_{p'+s}+i\eta},\end{aligned} \tag{29}$$

where $\epsilon_p=p^2$.

We integrate over q_0 and q_0' and thus obtain

$$\begin{aligned}\sigma_A^{(1)}(d)=&\frac{2e^2}{\omega c}\frac{1}{(2\pi)^6}\frac{\Omega}{(2\pi)^3}\int d\mathbf{p}'d\mathbf{s}(\mathbf{e}\cdot\mathbf{p}')[\mathbf{e}\cdot(\mathbf{p}'+\mathbf{s})]\\&\times\theta_F(\mathbf{p}')\theta_F(\mathbf{p}'+\mathbf{k})\theta_F(\mathbf{p}'+\mathbf{k}+\mathbf{s})\\&\times\bar{\theta}_F(\mathbf{p}'+\mathbf{s})(2\pi i)^2 i\int ds_0U(\mathbf{s},s_0)\\&\times\frac{1}{s_0-\epsilon_{p'+s}+\epsilon_{p'}-i\eta}\frac{1}{s_0-\epsilon_{p'+s}+\epsilon_{p'+k}-\omega-i\eta}\\&\times\frac{1}{\epsilon_{p'+k+s}-\epsilon_{p'+s}-\omega-i\eta}.\end{aligned} \tag{30}$$

Since

$$\omega-\epsilon_{p'+k+s}+\epsilon_{p'+s}\approx\omega[1-\omega/2mc^2-(p'+s)/mc]$$

cannot vanish, we can omit the $i\eta$ in the denominator of the last term in the right-hand side of Eq. (65). We now carry out the integration over s_0. The integrand has two poles in the s_0 plane and a cut arising from $U(\mathbf{s},s_0)$. These are shown in Fig. 9. We rotate the path of integration of s_0 by 90°, thereby performing the integration along the imaginary axis $i\zeta$. This will give, as one contribution to the cross section (the possible contribution from the intervening pole will be considered below),

$$\begin{aligned}\bar{\sigma}^{(1)}(d)=2\,\mathrm{Re}\sigma_A^{(1)}(d)\propto 2\,\mathrm{Re}\int_{-\infty}^{+\infty}id\zeta V(\mathbf{s},i\zeta)\\\times\frac{1}{i\zeta+\epsilon_{p'}-\epsilon_{p'+s+k}}\frac{1}{i\zeta+\epsilon_{p'+k}-\epsilon_{p'+s}-\omega},\end{aligned}$$

where $iV(\mathbf{s},i\zeta)=U(\mathbf{s},i\zeta)$. It has, furthermore, been proved[8] that $V(\mathbf{s},i\zeta)$ is a real number, and also that $V(\mathbf{s},i\zeta)=V(\mathbf{s},-i\zeta)$. Since the real part of the integrand in the equation for $\bar{\sigma}^{(1)}(d)$ is an odd function of ζ, we immediately arrive at the conclusion that the contribution from the integration over the $i\zeta$ axis gives identically zero. The only nonzero contribution results therefore from the pole in the first quadrant. $\sigma^{(1)}(d)$ is therefore given by

$$\begin{aligned}\sigma^{(1)}(d)=&\frac{2e^2}{\omega c}\frac{1}{(2\pi)^6}\frac{\Omega}{(2\pi)^3}2(2\pi)^3\int d\mathbf{p}'d\mathbf{s}(\mathbf{e}\cdot\mathbf{p}')[\mathbf{e}\cdot(\mathbf{p}'+\mathbf{s})]\\&\times\theta_F(\mathbf{p}')\theta_F(\mathbf{p}'+\mathbf{k})\theta_F(\mathbf{p}'+\mathbf{k}+\mathbf{s})\\&\times\bar{\theta}_F(\mathbf{p}'+\mathbf{s})\ \mathrm{Im}V(\mathbf{s},\,\omega-\epsilon_{p'+k}+\epsilon_{p'+s})\\&\times\frac{1}{\omega-\epsilon_{p'+k}+\epsilon_{p'}}\frac{1}{\omega-\epsilon_{p'+k+s}+\epsilon_{p'+s}},\end{aligned} \tag{31}$$

provided $\omega-\epsilon_{p'+k}+\epsilon_{p'+s}\gtrless 0$.

We next remark that some parts of Fig. 8 do not contribute to the cross section. We indicated at the

[8] N. Tzoar and A. Klein (unpublished).

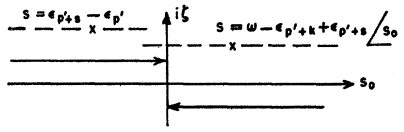

FIG. 9. Singularities of the integrand of Eq. (30).

beginning of this section that the contribution to the absorption cross section from a noninteracting electron gas vanishes. As was pointed out there, we have diagrams which represent nonphysical final states, i.e., final states which cannot simultaneously conserve energy and momentum. Those diagrams do not contribute to the cross section. A typical example is given in Fig. 8(c). In order to find the final state of the original absorption matrix element, we must cut the diagram by a horizontal line any place *between* the two crosses. If we then find an intermediate state which conserves energy and momentum, then this state can be real and corresponds to the final state in absorption. No such state can be found for this diagram. Following these instructions it is easily observed that diagrams 8(c) and 8(e) as well as diagram 10(c), etc., do not contribute to the absorption cross section inasmuch as they do not have an appropriate final state.

We record below the nonzero contributions to $\sigma(d)$, $\sigma(b)$, and $\sigma(c)$, as they are obtained from the diagrams of Figs. 8, 10, and 11, respectively. Let us first define the operators D and D_1,

$$D=\frac{2e^2}{\omega c}\frac{1}{(2\pi)^6}\frac{\Omega}{(2\pi)^3}2(2\pi)^3 \times\int d\mathbf{p}'d\mathbf{s}(\mathbf{e}\cdot\mathbf{p}')[\mathbf{e}\cdot(\mathbf{p}'+\mathbf{s})], \quad (32)$$

$$D_1=\frac{2e^2}{\omega c}\frac{1}{(2\pi)^6}\frac{\Omega}{(2\pi)^3}2(2\pi)^3\int d\mathbf{p}'d\mathbf{s}(\mathbf{e}\cdot\mathbf{p}')(\mathbf{e}\cdot\mathbf{p}'). \quad (33)$$

Similarly, we define the functions F_1 and F_2 (one must have always in mind that the energy argument of V must be greater than zero):

$$F_1=\frac{1}{\omega-\epsilon_{p'+k}+\epsilon_{p'}}\frac{1}{\omega-\epsilon_{p'+k+s}+\epsilon_{p'+s}} \times\mathrm{Im}V(\mathbf{s},\omega-\epsilon_{p'+k}+\epsilon_{p'+s}), \quad (34)$$

$$F_1'=\frac{1}{(\omega-\epsilon_{p'+k}+\epsilon_{p'})^2}\mathrm{Im}V(\mathbf{s},\omega-\epsilon_{p'+k}+\epsilon_{p'+s}), \quad (35)$$

$$F_2=\frac{1}{\omega-\epsilon_{p'+k}+\epsilon_{p'}}\frac{1}{\omega-\epsilon_{p'+k+s}+\epsilon_{p'+s}} \times\mathrm{Im}V(\mathbf{s},\omega-\epsilon_{p'+k+s}+\epsilon_{p'}), \quad (36)$$

$$F_2'=\frac{1}{(\omega-\epsilon_{p'+k}+\epsilon_{p'})^2}\mathrm{Im}V(\mathbf{s},\omega-\epsilon_{p'+k+s}+\epsilon_{p'}). \quad (37)$$

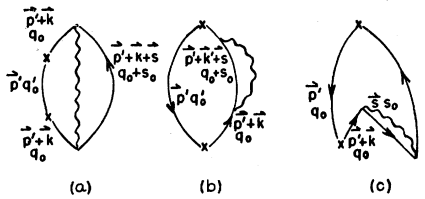

FIG. 10. Time-ordered contributions corresponding to Fig. 7(b).

We can thus write for the cross section

$$\sigma^{(1)}(d)=D\{\theta_F(\mathbf{p}')\theta_F(\mathbf{p}'+\mathbf{k}) \times\theta_F(\mathbf{p}'+\mathbf{k}+\mathbf{s})\bar{\theta}_F(\mathbf{p}'+\mathbf{s})F_1\}, \quad (38)$$

$$\sigma^{(2)}(d)=D\{\theta_F(\mathbf{p}')\theta_F(\mathbf{p}'+\mathbf{k}) \times\bar{\theta}_F(\mathbf{p}'+\mathbf{k}+\mathbf{s})\bar{\theta}_F(\mathbf{p}'+\mathbf{s})F_1\}, \quad (39)$$

$$\sigma^{(4)}(d)=D\{\theta_F(\mathbf{p}'+\mathbf{k})\theta_F(\mathbf{p}'+\mathbf{k}+\mathbf{s}) \times\theta_F(\mathbf{p}'+\mathbf{s})\bar{\theta}_F(\mathbf{p}')F_2\}, \quad (40)$$

$$\sigma^{(6)}(d)=D\{\theta_F(\mathbf{p}'+\mathbf{s})\theta_F(\mathbf{p}'+\mathbf{k}+\mathbf{s}) \times\bar{\theta}_F(\mathbf{p}')\bar{\theta}_F(\mathbf{p}'+\mathbf{k})F_2\}, \quad (41)$$

$$\sigma^{(7)}(d)=D\{\theta_F(\mathbf{p}'+\mathbf{k})\theta_F(\mathbf{p}'+\mathbf{k}+\mathbf{s}) \times\bar{\theta}_F(\mathbf{p}'+\mathbf{s})\bar{\theta}_F(\mathbf{p}')[F_1+F_2]\}, \quad (42)$$

$$\sigma^{(8)}(d)=D\{\theta_F(\mathbf{p}'+\mathbf{k})\bar{\theta}_F(\mathbf{p}'+\mathbf{k}+\mathbf{s}) \times\bar{\theta}_F(\mathbf{p}'+\mathbf{s})\bar{\theta}_F(\mathbf{p}')F_1\}, \quad (43)$$

$$\sigma^{(9)}(d)=D\{\theta_F(\mathbf{p}'+\mathbf{k}+\mathbf{s})\bar{\theta}_F(\mathbf{p}'+\mathbf{s}) \times\bar{\theta}_F(\mathbf{p}'+\mathbf{k})\bar{\theta}_F(\mathbf{p}')F_2\}, \quad (44)$$

$$\sigma^{(1)}(b)=-D_1\{\theta_F(\mathbf{p}'+\mathbf{k}+\mathbf{s}) \times\bar{\theta}_F(\mathbf{p}')\bar{\theta}_F(\mathbf{p}'+\mathbf{k})F_2'\}, \quad (45)$$

$$\sigma^{(2)}(b)=-D_1\{\theta_F(\mathbf{p}'+\mathbf{k}) \times\theta_F(\mathbf{p}'+\mathbf{k}+\mathbf{s})\bar{\theta}_F(\mathbf{p}')F_2'\}, \quad (46)$$

$$\sigma^{(1)}(c)=-D_1\{\theta_F(\mathbf{p}'+\mathbf{k})\bar{\theta}_F(\mathbf{p}')\bar{\theta}_F(\mathbf{p}'+\mathbf{s})F_1'\}, \quad (47)$$

$$\sigma^{(2)}(c)=-D_1\{\theta_F(\mathbf{p}')\theta_F(\mathbf{p}'+\mathbf{k})\bar{\theta}_F(\mathbf{p}'+\mathbf{s})F_1'\}. \quad (48)$$

We simplify this result by observing that in the dipole approximation where $k\ll p_F$ we have

$$\frac{1}{\omega-\epsilon_{p'+k}+\epsilon_{p'}}\approx\frac{1}{\omega};\quad\frac{1}{\omega-\epsilon_{p'+k+s}+\epsilon_{p'+s}}\approx\frac{1}{\omega}.$$

This implies $F_1=F_1'$ and $F_2=F_2'$. We also can in the dipole approximation put $\mathbf{p}'+\mathbf{k}\rightarrow\mathbf{p}'$, and $\mathbf{p}'+\mathbf{k}+\mathbf{s}\rightarrow\mathbf{p}'+\mathbf{s}$, which is equivalent to setting $\mathbf{k}=0$ in the equation for σ. We next sum over those terms which contain F_1, and separately over those which contain F_2. In the

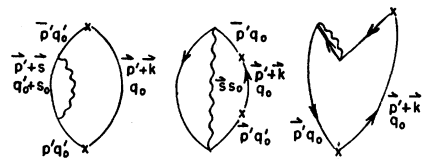

FIG. 11. Time-ordered contributions corresponding to Fig. 7(c).

terms containing F_1 we perform a change of variables, $\mathbf{p}'\rightarrow\mathbf{p}'-\mathbf{s}$, $\mathbf{s}\rightarrow-\mathbf{s}$. As a consequence we obtain the final result of this section:

$$\sigma=\sigma_{\text{total}}=\frac{2e^2}{\omega c}\frac{1}{(2\pi)^6}\frac{\Omega}{(2\pi)^3}2(2\pi)^3\int d\mathbf{p}'d\mathbf{s}\bar{\theta}_F(\mathbf{p}')\theta_F(\mathbf{p}'+\mathbf{s})$$
$$\times\frac{1}{\omega^2}[(\mathbf{e}\cdot\mathbf{p}')[\mathbf{e}\cdot(\mathbf{p}'+\mathbf{s})]+(\mathbf{e}\cdot\mathbf{p}')[\mathbf{e}\cdot(\mathbf{p}'+\mathbf{s})]$$
$$-(\mathbf{e}\cdot\mathbf{p}')^2-[\mathbf{e}\cdot(\mathbf{p}'+\mathbf{s})]^2]\,\mathrm{Im}V(\mathbf{s},\omega-\epsilon_{p'+s}+\epsilon_{p'})$$
$$=-\frac{2e^2}{\omega c}\frac{1}{(2\pi)^6}\frac{\Omega}{(2\pi)^3}2(2\pi)^3\frac{1}{\omega^2}\int d\mathbf{p}'d\mathbf{s}\,\bar{\theta}_F(\mathbf{p}')$$
$$\times\theta_F(\mathbf{p}'+\mathbf{s})(\mathbf{e}\cdot\mathbf{s})^2\,\mathrm{Im}V(\mathbf{s},\omega-\epsilon_{p'+s}+\epsilon_{p'}),\quad(49)$$

where

$$\omega-\epsilon_{p'+s}+\epsilon_{p'}\geqslant 0.$$

We conclude this section by summarizing our results. The random-phase approximation which allows us to excite only a plasmon does not contribute to the absorption cross section. This can be understood inasmuch as the plasmon is a longitudinal mode of vibration and as such the transverse photon does not couple directly to it. The next approximation for the dense electron gas is given by the diagrams in Figs. 7(b)–(d). This describes the virtual creation of a pair by absorption of a photon, thereafter decaying to the final state of pair plus plasmon or two pairs. We consider in detail only the former possibility. Now for any given plasmon there are many pairs in the electron gas, which together with the plasmon will conserve energy and momentum in the absorption of a photon. Therefore we find that there are many possible final states resulting from the photon absorption. We thus conclude that in the case of the electron gas we will not get a sharp resonance line even with the approximation that we keep only the plasmon part of the effective interaction. The width of the absorption cross section, as we shall calculate in the following section, does not result from a finite lifetime of a particular final state. Its actual origin will be described in the discussion at the end of the following section. There we will compute the cross section for the case where we assume the plasmon to be a bound state of the system. A more accurate calculation must take into account the finite lifetime of the plasmon itself.

III. EVALUATION OF THE ABSORPTION CROSS SECTION

In the preceding section we obtained the absorption cross section for the absorption of electromagnetic radiation by a dense electron gas. We saw that the electric field of the photon represented by the polarization vector $\mathbf{e}$ is coupled to the plasmon momentum. In order to evaluate this cross section simply we shall confine ourselves to the approximation that the plasmon is a bound state of the system. This approximation is necessary if we wish to avoid machine calculations which are hardly justified at the present stage of development of our theory. This approximation should preserve the main characteristic of the real solution where the plasmon has a sharp peak at the plasmon frequency. The function $\sigma(\omega)$ which we shall obtain in our calculation will exhibit a peak with a width smaller than the real one since we do not take into account the finite lifetime of the plasmon state.

We first write

$$V(\mathbf{s},\omega-\epsilon_{p+s}+\epsilon_p)=\frac{4\pi e^2}{s^2K(\mathbf{s},\omega-\epsilon_{p+s}+\epsilon_p)},\quad(50)$$

where K is the effective dielectric constant.[9] The cross section is thus given by

$$\sigma=-\sigma_0\int\frac{d\mathbf{p}d\mathbf{s}}{p_F{}^6}\bar{\theta}_F(\mathbf{p})\theta_F(\mathbf{p}+\mathbf{s})$$
$$\times(\mathbf{e}\cdot\hat{s})^2\,\mathrm{Im}\frac{1}{K(\mathbf{s},\omega-\epsilon_{p+s}+\epsilon_p)},\quad(51)$$

where

$$\sigma_0=(2e^2/c)(2\pi)^{-6}(2\Omega)(4\pi e^2)\omega^{-3}p_F{}^6.\quad(52)$$

If we use the well-known relations connecting the Fermi momentum, the classical plasmon frequency, and the density,

$$\Omega=(N/\rho),\quad 8\pi e^2\rho=\Omega_p{}^2,\quad \rho=(p_F{}^3/3\pi^2),$$

we then obtain for the cross section

$$\sigma=-Ax^2\frac{1}{\eta^3}\int d\mathbf{q}d\boldsymbol{\zeta}\,(\mathbf{e}\cdot\hat{s})^2\bar{\theta}_F(\mathbf{q})$$
$$\times\theta_F(\mathbf{q}+\boldsymbol{\zeta})\,\mathrm{Im}\frac{1}{K(\mathbf{s},\omega-\epsilon_{p+s}+\epsilon_p)},\quad(53)$$

where

$$A=(q/32\pi^2)(e^2/cp_F{}^2)N,$$
$$\eta=(\omega/p_F{}^2),\quad x=(\Omega_p/p_F{}^2),\quad(54)$$
$$\mathbf{q}=(\mathbf{p}/p_F),\quad \boldsymbol{\zeta}=(\mathbf{s}/p_F).$$

Since the momentum and energy in $K(\mathbf{k},k_0)$ are normalized to p_F and $p_F{}^2$, respectively, we now approximate $\mathrm{Im}(1/K)$ by the delta function,

$$-\pi\delta([\omega-\Omega_p(s)-\epsilon_{p+s}+\epsilon_p]/p_F{}^2).$$

Finally we substitute for the plasmon frequency $\Omega_p(s)$ its value at $s=0$, thus giving $\Omega_p(s)\approx\Omega_p$, since we know that $\Omega_p(s)$ is a slowly varying function of s. With all previous approximations we arrive at the equation

$$\sigma=\pi Ax^2\frac{1}{\eta^3}\int d\mathbf{q}d\boldsymbol{\zeta}\,(\mathbf{e}\cdot\boldsymbol{\zeta}/\zeta)^2\bar{\theta}_F(\mathbf{q})\theta_F(\mathbf{q}+\boldsymbol{\zeta})$$
$$\times\delta(\rho-\zeta^2-2\boldsymbol{\zeta}\cdot\mathbf{q}),\quad(55)$$

[9] R. A. Ferrell, Phys. Rev. **107**, 450 (1957); D. F. DuBois, Ann Phys. **7**, 174 (1959); **8**, 24 (1959).

where $\rho=\eta-x$. Since $\zeta^2+2\boldsymbol{\zeta}\cdot\mathbf{q}\geqslant 0$, we have a contribution to σ only if $\rho\geqslant 0$ or $\eta\geqslant x$ which implies $\omega\geqslant\Omega_p$.

The integration of σ is a straightforward calculation which can be given in explicit form only if one specifies a value for x. We therefore proceed to a numerical calculation for a particular choice, $x=2$, since theoretical calculations as well as experimental results, in different metals of interest,[10] indicate this as an average value for x.

We thus obtain (for $x=2$, i.e., $\rho=\eta-2$)

$$\sigma=\sigma_0\frac{1}{\eta^3}\left[[\eta-\tfrac{1}{8}(\gamma^2+\beta^2)](\gamma^2-\beta^2)-\frac{(\eta-2)^2}{2}\ln\frac{\gamma}{\beta}+(\eta-2)(\alpha^2-\gamma^2)\right] \quad (56)$$

for $3\geqslant\eta\geqslant 2$, and

$$\sigma=\sigma_0\frac{1}{\eta^3}\left[[\eta-\tfrac{1}{8}(\alpha^2-\beta^2)](\alpha^2-\beta^2)-\frac{(\eta-2)^2}{2}\ln\frac{\alpha}{\beta}\right] \quad (57)$$

for $\eta\geqslant 3$, where

$$\begin{aligned}\alpha&=(\eta+1)^{\frac{1}{2}}-1,\\ \beta&=(\eta-1)^{\frac{1}{2}}-1,\\ \gamma&=1-(3-\eta)^{\frac{1}{2}},\\ \sigma_0&=(4\pi^3/12)Ax^2.\end{aligned} \quad (58)$$

The cross section as a function of η is plotted in Fig. 12 and its general features discussed below.

To understand the nature of the curve of Fig. 12 that we have obtained for the total cross section, we write symbolically

$$\sigma(\omega)\propto|\text{matrix element}|^2\times\int(\text{allowed phase space}). \quad (59)$$

The allowed phase space is given by

$$\int d\mathbf{q}d\boldsymbol{\zeta}(\mathbf{e}\cdot\hat{s})^2\bar{\theta}_F(\mathbf{q})\theta_F(\mathbf{q}+\boldsymbol{\zeta})\delta(\rho-(\mathbf{q}+\boldsymbol{\zeta})^2+q^2)$$

which immediately implies a threshold for the photon energy at $\rho=\eta-x=0$. We thus can say that in our approximation an absorption of γ rays is possible only for $\omega\geqslant\Omega_p$. At the value $\omega=\Omega_p$, i.e., $\rho=0$, we obtain $\sigma(\omega=\Omega_p)=0$. This can be easily observed from Eq. (55). Then by carrying out a detailed but straightforward calculation, we arrive at the conclusion that $(d/d\eta)\times\int$(allowed phase space) is greater than zero at $\eta=x$, and for the limit $\eta\to\infty$, $\int$(allowed phase space)$\propto\eta$. Since, as we will see below, the |matrix element|^2 is proportional to η^{-3}, we obtain for σ a curve which increases steeply when ω exceeds Ω_p and then drops to zero as η^{-2} for $\eta\to\infty$.

[10] For information about the plasma frequency for different metals, see D. Pines, in *Solid-State Physics*, edited by F. Seitz and D. Turnbull (Academic Press, Inc., New York, 1955).

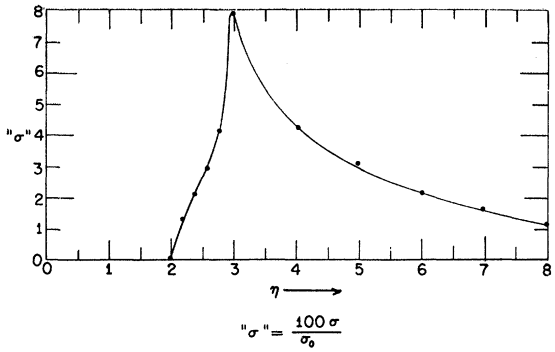

FIG. 12. Total absorption cross section for photons vs photon energy. Here $\eta=\omega/p_F^2$ is the ratio of photon energy to Fermi energy. The curve drawn is for the special case $(\Omega_p/p_F^2)=2$, where Ω_p is the classical plasmon frequency.

We now show the origin of the energy dependence of the |matrix element|^2 by analyzing as a typical example the contribution from the diagram given in Fig. 8g). The energy dependence, as in the case of time-dependent perturbation theory, appears for any intermediate state as a denominator equal to the photon energy minus the excitation energy. In the case of an intermediate state not containing a plasmon, the intermediate energy is zero in the dipole approximation, i.e., when $\mathbf{k}=0$. Therefore, we obtain a factor of ω^{-1} for any intermediate state without a plasmon. The intermediate state containing the plasmon will contribute to the delta function which dictates the energy conservation in the final state. Since any interaction with a photon contributes to the matrix element a factor of $\omega^{-\frac{1}{2}}$, we finally obtain |matrix element|$^2\propto\omega^{-3}$ as was indicated before. We would thus conclude that the peak in the absorption cross section is due to the rapid increase of the phase space immediately above the threshold energy ($\omega=\Omega_p$), and the fast decrease of the cross section by the factor of η^{-2} in the high-energy region.

In conclusion, we wish to emphasize that an experimental check of our theory, or of a suitable modification thereof to apply to real metals, would test an aspect of the concept of the plasmons in the high-density limit which goes beyond the usual random-phase approximation.

IV. CONCLUSIONS

In the previous pages we calculated the absorption cross section for a photon by an electron gas in the high-density limit. In particular we were interested in finding the mechanism by which the electromagnetic field can be coupled to a plasmon and in computing the cross section arising from this process. This process is initiated by a virtual pair, excited by the photon, thereafter decaying to a final pair plus a plasmon. Since for a given plasmon we have many pairs which together with the

TABLE I. Fermi energies and plasma frequencies of typical metals.

Metal	ϵ_F (ev)	Ω_p (ev)
Cu	7.04	11.00
Ag	5.51	9.00
Au	5.54	9.00
Si	11.7	17.00

plasmon conserve energy and momentum we do not obtain a sharp absorption line. Rather, we obtain a threshold in the cross section at photon energy equal to the plasmon energy Ω_p. Then the cross section increases to a peak at a photon energy equal roughly to $\Omega_p+\epsilon_F$, where ϵ_F is the Fermi energy. At photon energies ω higher than $\Omega_p+\epsilon_F$ the cross section behaves as ω^{-2}.

We now argue that if the electromagnetic field can excite a plasmon through the mechanism proposed here, one should be able to detect it experimentally, since the cross section per electron, which emerges from our formula when one inserts realistic densities, is of the order of magnitude of $10^{-17}-10^{-19}$ cm^2. The experiment should be carried out with a thin foil in order to eliminate reflection losses (a thickness of the order of 10^3 A will still preserve the many-body characteristics of the electron gas). Moreover, interband transitions and other losses cause a cross section per electron of about $10^{-17}-10^{-20}$ cm^2. Detection and separation of the effect discussed here is therefore not out of the question.

ACKNOWLEDGMENTS

One of the authors (N.T.) would like to thank Dr. R. Amado, Dr. E. Burstein, Dr. M. Cohen, and Dr. J. Luttinger for helpful discussions.